Original Article

MEDICINE PALLIATIVE CARE

DOI: 10.47582/jompac.1865602

J Med Palliat Care. 2026;7(2):391-400

Fast-disintegrating under-eye mask: postbiotic-loaded polyvinylpyrrolidone nanofibers for anti-aging and hydration application

Muhammet Sait Toprak[1,2,3], Ece Güler[2,3,4], Hümeyra Betül Yekeler[2,3,5], Gülsüm Ercan[2,3,6,7], Deniz Baybağ[2], Aleyna Çavdar[2,8], Nedim Can Çevik[2], Muhammet Emin Çam*[2,3,4,9]

[1]*Department of Biochemistry, Faculty of Pharmacy, İstanbul Kent University, İstanbul, Turkiye*
[2]*ResearchKent, İstanbul Kent University, İstanbul, Turkiye*
[3]*MecNano Technologies, Cube Incubation, Teknopark İstanbul, İstanbul, Turkiye*
[4]*Department of Pharmacology, Faculty of Pharmacy, İstanbul Kent University, İstanbul, Turkiye*
[5]*Department of Pharmacology, Faculty of Pharmacy, Marmara University, İstanbul, Turkiye*
[6]*Department of Pharmaceutical Technology, Faculty of Pharmacy, İstanbul Kent University, İstanbul, Turkiye*
[7]*Department of Pharmaceutical Technology, Faculty of Pharmacy, University of Health Sciences, İstanbul, Turkiye*
[8]*Department of Bioengineering, Faculty of Chemical and Metallurgical Engineering, Yıldız Technical University, İstanbul, Turkiye*
[9]*Shymeriae Biotechnology, İstanbul, Turkiye*

Cite this article as: Toprak MS, Güler E, Yekeler HB, et al. Fast-disintegrating under-eye mask: postbiotic-loaded polyvinylpyrrolidone nanofibers for anti-aging and hydration application. *J Med Palliat Care*. 2026;7(2):391-400. doi:10.47582/jompac.1865602

Received: 17.01.2026 • **Accepted**: 25.03.2026 • **Published**: 27.03.2026

ABSTRACT

Aims: The aim of this study was to develop and characterize postbiotic-loaded polyvinylpyrrolidone (PVP) nanofibers (PBNF) as a fast-disintegrating under-eye delivery system and to investigate their in vitro performance, including physicochemical properties, release kinetics, biocompatibility, and their potential to modulate skin-related cellular and molecular responses.

Methods: PBNFs containing 0.5%, 1%, and 1.5% postbiotics were fabricated using pressurized gyration (PG) technology. Pure nanofibers (PNF) served as controls. The nanofibers were characterized for morphology (SEM), chemical structure (FTIR), encapsulation efficiency, dissolution behavior, release kinetics, and disintegration properties. In vitro biological performance was assessed using L929 fibroblast and HaCaT keratinocyte cells through WST-1 viability assays and morphological analysis. Additionally, gene expression analysis was performed by qPCR to evaluate the molecular effects of the formulations on extracellular matrix remodeling and inflammatory markers.

Results: SEM analysis revealed uniform, bead-free nanofibers with comparable diameters across all formulations, indicating that postbiotic loading did not alter fiber morphology. FTIR spectra confirmed the successful incorporation of postbiotics into the PVP matrix. Among the formulations, 0.5% PBNF exhibited the highest encapsulation efficiency and was selected for further evaluation. Dissolution studies demonstrated a rapid initial release followed by diffusion-controlled kinetics best described by the Higuchi model. Disintegration tests showed ultrafast wetting and dissolution of the nanofibers in PBS within seconds. In vitro studies demonstrated that PBNFs promoted cell viability and proliferation in a dose- and time-dependent manner, resulting in a more balanced and controlled biological response compared to free postbiotics or PNF, without inducing cytotoxic effects. qPCR analysis demonstrated a coordinated modulation of extracellular matrix-related genes, characterized by decreased MMP1 and increased COL1A1 expression in PBNF groups, while IL6 levels remained stable.

Conclusion: PBNF produced by PG represents a biocompatible, fast-disintegrating, and effective topical delivery system with strong potential for use in under-eye cosmetics and regenerative applications.

Keywords: Postbiotic, nanofiber, pressurized gyration, anti-aging, hydration, under-eye mask

INTRODUCTION

Skin is the human body's largest organ and serves as the primary defense mechanism against the environment. It is a crucial component of the innate immune system and functions as a physical barrier. The skin plays many important roles, including regulating water loss from the body, preventing infection, regulating body temperature, providing the sense of touch, and producing vitamin D.[1,2]

With increasing age, there is a progressive decrease in cutaneous collagen content, resulting in a loss of dermal elasticity, progressive folding or sagging, and the development

***Corresponding Author:** Muhammet Emin Çam, muhammet.cam@kent.edu.tr

of both superficial and deep wrinkles. As a function of increasing age, skin shows signs of aging more quickly than most other vital organs. The prevalence of aging-associated cutaneous diseases is increasing substantially and profoundly negatively affects the quality of life. Abnormal modifications in the composition of the cutaneous barrier have been assumed to be responsible for most cutaneous diseases, including those associated with aging. Thus, accelerating skin aging to improve the barrier function is of foremost significance.[3,4]

Current evidence suggests that age-related changes in both the skin and gut microbiota contribute to "inflammaging" and impaired skin homeostasis via the gut-skin axis. In recent years, probiotics, prebiotics, and postbiotics have emerged as potential modulators of skin aging. Probiotics, in particular, have garnered attention for their ability to modulate the gut-skin axis, reduce inflammation, and support skin rejuvenation.[5]

The definition of postbiotics is given as a non-viable form of microorganisms or their derived components, which in turn have positive effects on living organisms in a direct or indirect manner. A postbiotic can contain various active elements, including short-chain fatty acids, bacterial lysates, cell-free culture supernatants, cell wall constituents, enzymes, or exopolysaccharides. Although these possess different benefits for humans, the use of postbiotics is hindered by poor pharmacokinetic properties, low bioavailability, non-specific pharmacology, poor palatability, and unpleasant odor.[6]

Probiotics, prebiotics, and postbiotics modulate skin aging by restoring microbial balance, particularly through the gut-skin axis, enhancing barrier integrity, and regulating immune and oxidative pathways. Topical formulations exert their effects locally by strengthening tight junctions, increasing ceramide synthesis, and inhibiting inflammatory mediators and matrix metalloproteinases.[5]

The orbital region is frequently where signs of skin aging are most apparent, due to the extremely thin skin that characteristically presents in this area. The periorbital region exhibits signs of premature aging, in contrast to the rest of the face. The signs include the manifestation of hyperpigmentation, wrinkles, and the development of edema in the orbital region. The treatment currently in vogue includes topical preparations in the form of creams and lotions. The skin rejuvenation therapies employed to counteract the signs of aging in the periorbital region include those commercially sold in the form of orbital region skin masks, which work to counter the manifestations of edema, dryness, and wrinkles.[3,4]

Nanofibers in the nanometer scale are characterized by high surface area, high mechanical strength, high porosity, and an elastomeric structure. The nanofibers can effectively mimic the properties of the extracellular matrix in medical fields by combining natural and synthetic polymers. Nanofiber production is traditionally achieved mainly through electrospinning techniques, which involve a high electrostatic potential difference between the tip of the syringe and the collector to extrude a polymeric solution and form a nanofiber scaffold. Besides electrospinning techniques, other novel nanofibers produced by utilizing pressurized gyration (PG) technology offer improvements, including the very short time required to produce nanofibers, from solution deposition to reservoir, in approximately 1-2 seconds. Compared to other nanofiber fabrication techniques already in practice, PG technology introduces improvements in fabrication with lower electrical requirements and sterility during fabrication and significantly enhances production capacity and output to accommodate mass production in a conventional environment.[7]

Polyvinylpyrrolidone (PVP) is a hydrophilic polymer that is non-toxic in nature and has been approved by the FDA in various medical, pharmaceutical, food, and cosmetic applications. PVP can be described as an inert polymer, and it is biodegradable in nature, exhibiting stability at various temperatures and pH levels. In the cosmetic industry, PVP acts as an agent in removing facial fine lines, improving hydration, and promoting the production of anti-aging cosmetic products.[8,9]

The topic handled in this research paper is the fascinating and highly advanced topic of nanotechnology in relation to postbiotic delivery. Although the preliminary pre-clinical findings appear very optimistic, there is a conspicuous lack of information in the clinical setting, necessitating further development in the future. This research paper consists of two primary objectives. The first objective is to establish the utility of postbiotics in preventing under-eye wrinkles, while the second focuses on utilizing nanotechnology to enhance the targeted delivery of these molecules. Therefore, PVP nanofibers loaded with postbiotics were developed to achieve anti-aging and hydration effects, and their properties were characterized through various tests, thereby proving their nontoxic profile.

This study presents a novel integration of PG technology, postbiotic-loaded nanofibers, and a rapidly disintegrating hydrophilic PVP matrix for topical under-eye application. Compared to conventional electrospinning-based systems, PG offers superior scalability, production efficiency, and industrial applicability. Despite the growing interest in postbiotics, their incorporation into nanofiber-based delivery systems remains limited, particularly in formulations designed for periorbital use. To date, no scientific studies have reported the development of fast-disintegrating under-eye masks produced via PG using postbiotic-loaded nanofibers. Therefore, this study addresses this gap by proposing a novel formulation characterized by rapid disintegration, efficient release, and favorable biocompatibility, representing a distinct advancement over conventional sustained-release topical systems and existing eye care products.

METHODS

Ethics

Since this study involved the use of materials, approval from an ethics committee was not required.

Materials

PVP (PVP K30, molecular weight: 40,000 g mol^{-1}) was purchased from Sigma Aldrich. The postbiotic mixture was

obtained from Shymeriae Biotechnology (İstanbul, Turkiye). Phosphate buffer saline (PBS) tablets (pH 7.4) were bought from Chembio (İstanbul, Turkiye). WST-1 Assay Kit (ab65473) was purchased from Abcam (Cambridge, UK). Quick-RNA™ MiniPrep Kit (Cat. No: R1054) was purchased from Zymo Research (USA). cDNA Synthesis Kit (5X) purchased from NucleoGene (İstanbul, Turkiye). SensiFAST™ SYBR® No-ROX Kit was purchased from Bioline (Meridian Bioscience, USA). NCTC clone 929 (L cell, L-929, derivative of Strain L) CCL-1™ and HaCaT 300493; Cytion cells were used in this study.

Preparation of Solutions

PVP solution with a concentration of 100% (wt/v) was prepared by dissolving PVP in distilled water. PVP was added in fractional amounts to distilled water over a period of approximately 8 hours. On average, approximately 1.25 g of polymer was added per hour to 10 ml of distilled water, and continuous magnetic stirring was applied to prevent clumping. To facilitate dissolution, the ambient temperature was maintained at approximately 30 °C. Since the polymer was added slowly and in a controlled manner rather than all at once, a homogeneous and complete dissolution was achieved. Then, postbiotics were added to this 100% PVP solution in ratios of 0.5%, 1%, and 1.5%, resulting in the formation of nanofibers. The production of pure nanofibers (PNF) and 0.5, 1, and 1.5% postbiotics-loaded nanofibers (0.5 PBNF, 1 PBNF, and 1.5 PBNF, respectively) utilized the PG technique under the following settings: temperature, 26-36°C; pressure, 0.1-0.3 MPa; humidity level, 35-55%; and rotation speed, 17000 rpm.

Preparation of Postbiotics

Microorganism strains used for postbiotic production were selected from previously identified isolates that had been determined to exhibit suitable probiotic characteristics. The selected strains are *Lactobacillus acidophilus LTC-La060301, Bifidobacterium longum LTC-BSP1908, Lactobacillus fermentum LTC-LFM090197, Streptococcus thermophilus LTC-ST140700.*The microorganisms were inoculated at a rate of 1% (v/v) into an appropriate growth medium (e.g., de Man, Rogosa and Sharpe (MRS) broth) and incubated under controlled fermentation conditions. Fermentation was carried out at 37 °C under anaerobic conditions for 24–48 hours.[10] During fermentation, changes in culture pH were monitored, and the fermentation process was terminated when the pH reached a range of 4–5 and the viable cell count exceeded 1×10^9 CFU/ml.[11] At the end of fermentation, cultures were centrifuged at 6000×g for 30 min at 25 °C to separate microbial cells. The resulting supernatant was carefully collected and passed through 0.45 µm pore-size cellulosic membrane filters to completely remove residual cellular debris. This procedure yielded a cell-free supernatant devoid of viable microorganisms. The absence of live microorganisms in the supernatants was confirmed by inoculation onto appropriate culture media.[10,12] The obtained cell-free supernatants were considered as the postbiotic fraction and stored at 4 °C to preserve stability. Prior to experimental use, all samples were brought to room temperature.[13]

Scanning Electron Microscope (SEM)

The size and morphology of the nanofibers were examined using a (SEM, EVO LS 10, ZEISS). The surface of the samples was coated with gold for 120 seconds. The average nanofiber diameter and size distribution were determined by analyzing 100 nanofibers in randomly selected SEM micrographs using ImageJ (Brocken Symmetry Software).[14,15]

Fourier Transform Infrared Spectroscopy (FTIR)

The chemical structures of the compounds to be used in production and the carrier systems produced were analyzed using SHIMADZU IRSpirit-X. The interactions between these compounds were also investigated. Measurements were performed at room temperature, between 4000 and 450 cm^{-1}, in transmission mode with a resolution of 4 cm^{-1}. The spectrums were displayed using OPUS Viewer software version 6.5.[14,15]

Encapsulation Efficiency

To calculate the encapsulation efficiency (EE) of the nanofibers, the nanofibers were weighed to an average of 5 mg each and completely dissolved in 1 ml of solvent. After stirring for an average of 4 hours, the postbiotic loaded within the nanofibers was detected using a UV spectrophotometer at a wavelength of 363 nm.[16]

Dissolution Test

To evaluate the release profile of the drug-loaded nanofibers, three samples, each weighing 5 mg, were placed in an Eppendorf tube, and the release study was initiated. 1 ml of phosphate-buffered saline (PBS, pH 5.5) was added to the Eppendorf tubes and placed in a shaker water bath at room temperature. Subsequently, at specific time intervals (0, 1, 5, 10, 15, 30, 45, 90, 120, 150, and 180 seconds), the supernatant at the top of the Eppendorf tube was collected and measured spectrophotometrically at a specified wavelength. The same volume of fresh PBS was added to the nanofiber, which was placed in a shaking water bath, and the shaking process continued until the next measurement. As a result of this step, the absorbance values obtained from each supernatant were incorporated into the y part of the formula, and the amount of drug released, given by x in the formula, was calculated. The time-dependent amounts of drugs released were added up in order to obtain a cumulative release. A graph representing time-dependent release was used to study the kinetics of release.[14,15]

Drug Release Kinetics

In vitro simulations monitored the variation of drug levels in plasma over time. The amount of drugs released from nanofibers was fitted using five different mathematical models. Equations, which take into consideration the Korsmeyer-Peppas (1), zero-order (2), first-order (3), Higuchi (4), and Hixson-Crowell (5) models are given below with, respectively. The kinetic constants of these models are K, K_0, K_1, K_h, and K_{hc}, respectively. In these equations, Q represents the amount of the drug released in time t and n is the diffusion exponent.[17]

- $Q=Kt_n$ (1)
- $Q=K_0t$ (2)
- $In\ (1-Q)=-K_1t$ (3)
- $Q=K_ht^{1/2}$ (4)
- $Q^{1/3}=K_{hc}t$ (5)

Disintegration Test

A piece was cut from the fibers, approximately 3 cm in diameter, and placed in a Petri dish containing 15 ml of PBS (pH 5.5). The disintegration of the fibers was recorded at a speed of 50 frames per second using a video camera (Canon Sx70 HS, Tokyo, Japan).[18]

In vitro Cell Culture WST-1 Test

The WST-1 cell viability test is based on the principle that mitochondrial dehydrogenase enzymes in living cells reduce WST-1, a tetrazolium salt, to a water-soluble formazan product. The amount of formazan formed is directly proportional to the number of metabolically active cells in the culture and can be measured spectrophotometrically. This method offers advantages, particularly in nanomaterial and short-term toxicity studies, due to its lack of precipitation and solvent-free nature compared to the MTT test.

In the experiment, cells were seeded into 96-well plates at a rate of 5000 cells per well, and culture medium was added to each well to a total volume of 100 µL. To allow the cells to adhere to the surface and reach metabolic equilibrium, the plates were incubated for 24 hours in an incubator at 37 °C with 5% CO_2. After this period, the cells were separated into control and test groups at the appropriate concentrations, as specified in the experimental design. The relevant materials (postbiotic, pure nanofiber, and postbiotic-loaded nanofiber) were applied to the cells, and the cells were incubated for 6 and 24 hours. At the end of the incubation period, 10 µL of WST-1 reagent was added to each well, representing 10% of the available volume. Following the addition of the reagent, the plates were incubated for an hour in a light-free incubator at 37 °C and 5% CO_2.

After incubation, absorbance values were measured at a wavelength of 450 nm using a microplate reader. The obtained absorbance values were normalized to the control group to calculate the cell viability percentages. Results were expressed as the mean±standard deviation of at least three independent experiments, and statistically significant differences between groups were evaluated using appropriate statistical analysis methods.[19]

Gene Expression Analysis (qPCR)

Gene expression analysis was performed to evaluate the molecular effects of the developed formulations. Cells were seeded into 6-well plates at a density of 80,000 cells per well and incubated for 24 hours at 37 °C in a humidified atmosphere containing 5% CO_2 to allow for cell attachment and stabilization.

Following this incubation period, cells were treated with the specified concentrations of postbiotic, PNF, and PBNF according to the experimental design. After 24 hours of treatment, cells were harvested, and total RNA was isolated using a commercially available RNA isolation kit (Zymo Research) according to the manufacturer's instructions.

The isolated RNA was subsequently reverse-transcribed into complementary DNA (cDNA) using a cDNA synthesis kit (Bioline). Quantitative real-time PCR (qPCR) analysis was then performed using gene-specific primers to assess the expression levels of matrix metalloproteinase-1 (MMP1), collagen type-1 alpha-1 chain (COL1A1), cyclin-dependent kinase inhibitor-1A (CDKN1A), and interleukin 6 (IL6). Glyceraldehyde-3-phosphate dehydrogenase (GAPDH) was used as the housekeeping gene for normalization.

Thermal cycling conditions were applied according to standard qPCR protocols, with an annealing temperature of 57.5 °C. Relative gene expression levels were calculated using the comparative Ct (2^−ΔΔCt) method. All experiments were performed in at least three independent replicates.[20]

Statistical Analysis

The data analysis was performed using GraphPad Prism 9.0. The results were quoted as the mean±standard error of the mean, except for the fiber distribution graphs, which were presented as the mean±standard deviation (SD). A one-way ANOVA was performed in GraphPad Prism to compare group differences. The statistical significance of the results was determined based on the following p-value thresholds: $p<0.05$ indicates a statistically significant difference, $*p<0.01$ denotes a highly significant difference, and $*p<0.001$ represents a very highly significant difference.

RESULTS AND DISCUSSION

Scanning Electron Microscope (SEM)

SEM images of all samples and distribution histograms of nanofibers are shown in **Figure 1**. The results showed that the average nanofiber size distribution of PNF was 862±172 nm. After loading postbiotic, the diameters of 0.5 PBNF, 1 PBNF, and 1.5 PBNF were measured as 885±219, 775±284, and 835±275 nm, respectively. There was no correlation between the amount of postbiotic loaded and the diameter of the nanofibers. According to the results, the morphologies of the fibers were found to be similar to one another (**Figure 1**). Therefore, the best ratio of PBNF was chosen based on the EE results and was maintained at a ratio of 0.5 PBNF, which corresponded to the highest EE.

SEM analysis showed that postbiotic incorporation did not significantly affect the morphology or diameter of the PVP nanofibers. All formulations exhibited smooth, bead-free, and uniform structures, indicating that the PG process provided stable fiber formation conditions. The lack of correlation between postbiotic concentration and fiber diameter suggests that the addition of postbiotics did not markedly alter key parameters such as solution viscosity or polymer chain entanglement, which are critical for nanofiber formation.[7]

The preservation of fiber morphology following bioactive loading is consistent with previous studies demonstrating that the incorporation of active compounds does not necessarily compromise nanofiber structure when formulation parameters are well optimized.[4] Moreover, the uniform and

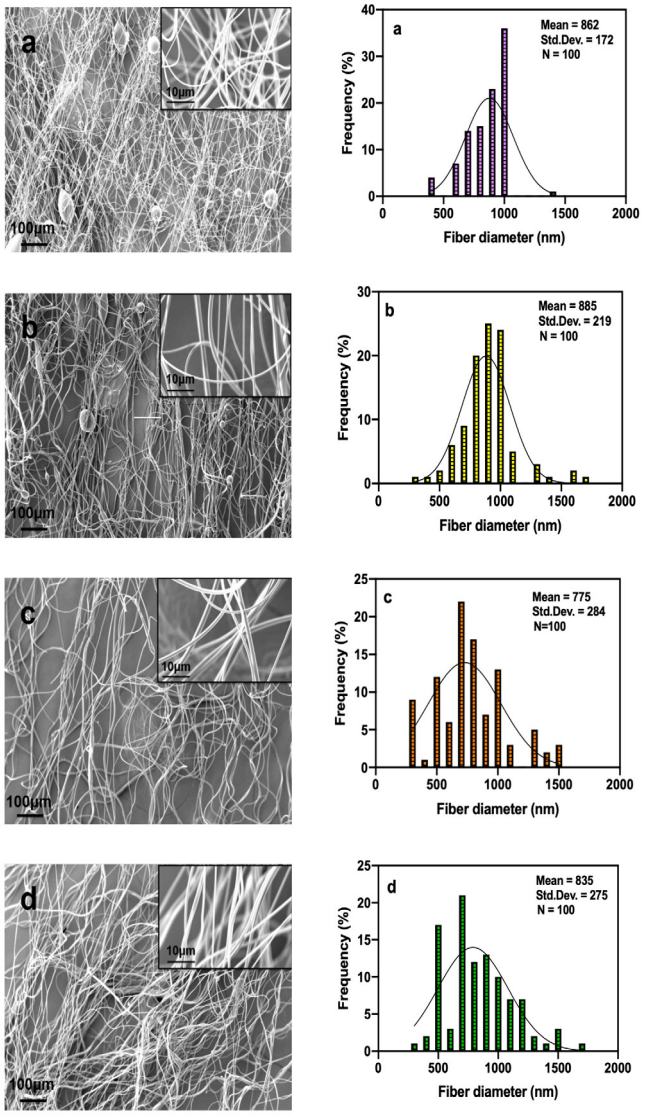

Figure 1. SEM images of (a) PNF, (b) 0.5 PBNF, (c) 1 PBNF, and (d) 1.5
PBNF. PBNF: Postbiotic-loaded nanofiber, PNF: Pure nanofiber

defect-free morphology observed across all groups reflects appropriate processing conditions and is known to be essential for ensuring reproducible release behavior and biological performance.[9]

Therefore, the selection of the 0.5% PBNF formulation based on its higher EE, while maintaining comparable morphological properties, supports its suitability for further evaluation.

Fourier Transform Infrared Spectroscopy (FTIR)

Figure 2 shows the peak absorptions of PNF and 0.5 PBNF. Examining the PVP spectrum, a broad O-H stretching peak is observed at 3401.8 cm^{-1}. The absorption at 2956.3 and 1645 cm^{-1} matches with CH_2 and C=O stretching, respectively. The bands at 1421.3 and 1286.3 cm^{-1} can be attributed to C-N stretching and CH_2 bending, respectively. Other absorption bands at 566-646 cm^{-1} can be attributed to N-C=O bending, in accordance with Guler et al.[21] The absorption peak at 3305.3 cm^{-1} in the case of 0.5 PBNF corresponds to the O-H stretching vibration. An absorption band at 1635.3 cm^{-1} can be assigned to the C=O stretching vibration.[22] Hence, all these absorption bands establish the successful incorporation of postbiotics into PNF.

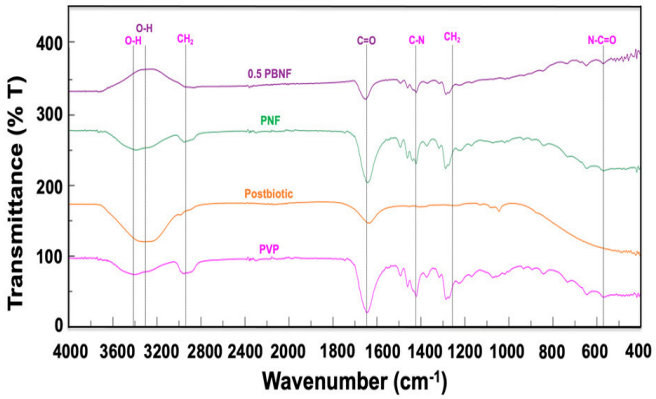

Figure 2. FTIR spectra of PVP, postbiotic, PNF, and 0.5 PBNF
PBNF: Postbiotic-loaded nanofiber, PNF: Pure nanofiber

Dissolution Test and Drug Release Kinetics

The dissolution test was performed to analyze the release profile of postbiotics in 0.5 PBNF. A linear standard calibration graph with a correlation coefficient of 0.9839 was obtained using UV absorption measurements in the range of postbiotics from 2 to 10 µg/ml (Figure 3a). The release of postbiotics was measured using UV absorption at 363 nm. The EE measurements of 0.5 PBNF, 1 PBNF, and 1.5 PBNF were obtained at 53.90%, 21.02%, and 27.42%, respectively (Figure 3b). According to these results, the analyses were continued with 0.5 PBNF due to its highest encapsulation rate. Then, the dissolution test of PBNF was performed over 180 seconds (Figure 3c). A burst release of postbiotics from nanofibers occurred within the first 45 seconds (52.89%), followed by 70.21% and 84.84% release within 90 and 120 seconds, respectively.

The release profiles were performed based on different kinetic models, including Korsmeyer-Peppas, Zero Order, First Order, Higuchi, and Hixson-Crowell. However, a higher goodness-of-fit analysis was achieved using the Higuchi model, as evident from the higher R^2 values plotted in Figure 3B. The release profile, as predicted by the Higuchi model in this study, reveals that the release of the postbiotic from the PVP nanofiber matrix is largely diffusion-controlled. As mentioned in the study cited, the Higuchi model represents matrix formulations wherein the drug of interest is evenly distributed and released based on a concentration gradient relative to the sink. In the case of the current formulation, the strong hydrophilic nature and rapid hydration of PVP, along with its high surface area and porous nanofiber structure, facilitate rapid solvent diffusion and, consequently, rapid diffusion-mediated release of the postbiotic. Consequently, although the nanofibers depolymerize quickly in the PBS solution, the release profile remains diffusion-controlled, as would be expected based on the underlying principles of the Higuchi model.[23]

Disintegration Test

The aim of the experiment was to establish the time of disintegration of the fibers. A 5-g weight of fibers was cut and added to the PBS solution using a thermal shaker. The

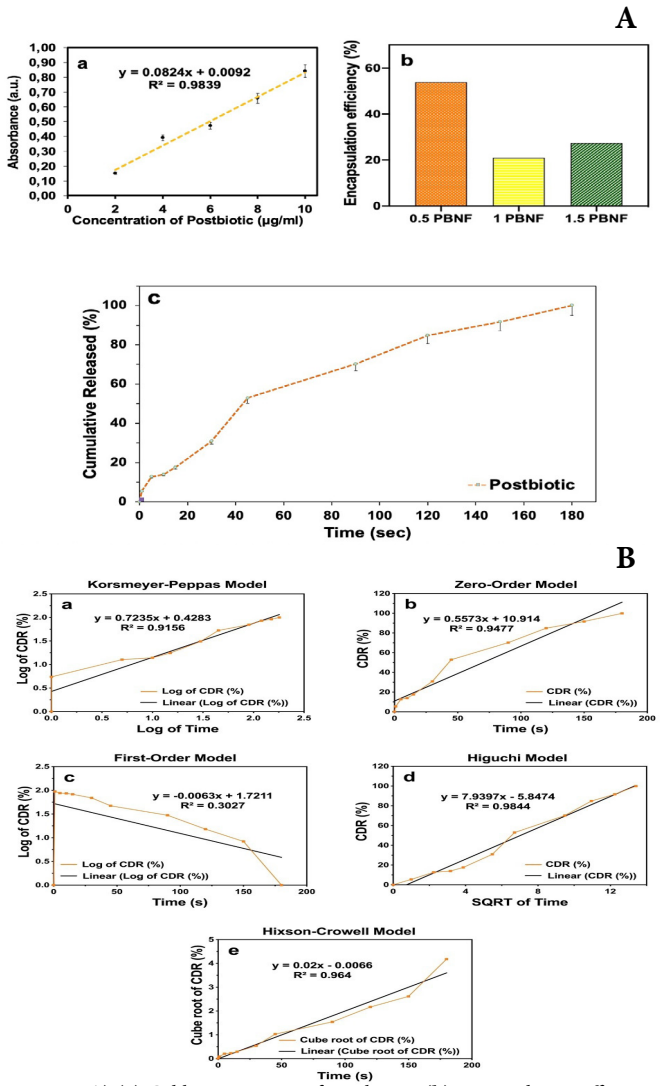

Figure 3. A) (**a**) Calibration curve of postbiotic, (**b**) encapsulation efficiency of postbiotic at different ratios, and (**c**) postbiotic cumulative release profile; **B**) Kinetic models of postbiotic release from nanofibers incubated in dynamic conditions in PBS (pH 5.5) at 32 °C: (**a**) Korsmeyer-Peppas, (**b**) zero-order, (**c**) first-order, (**d**) Higuchi, and (**e**) Hixson-Crowell mathematical methods
CDR: Cumulative drug release, SQRT: Square root

fiber wetted in less than 1 second and dissolved in less than 4 seconds. NF patches disintegrated in less than 3 seconds in the PBS solution due to their porous nature and high surface area. Fast-disintegrating NF systems have been demonstrated in the literature to be applicable in the transdermal and cosmetic fields due to their rapid wetting properties, which allow for the immediate release of biologically active substances. Images of the fiber disintegration can be found in Figure 4.[24]

WST-1 & Morphological Analysis

The cytotoxicity and proliferation data obtained in the present study collectively support the biocompatible nature of all tested formulations; however, the PBNFs emerged as the most biologically favorable construct, a finding that warrants mechanistic interpretation beyond simple viability comparisons.[25]

The transient and concentration-dependent decrease in cell viability observed at 24 hours, particularly at higher

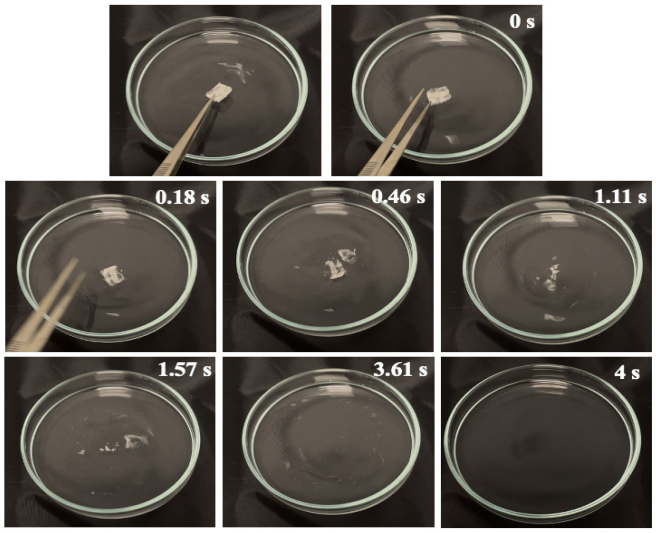

Figure 4. Disintegration and wetting test of PBNF within 4 seconds
PBNF: Postbiotic-loaded nanofiber

concentrations, is consistent with previously reported adaptive stress responses triggered by initial contact with polymeric nanofiber surfaces. Short-term viability reductions of this nature have been documented in studies employing electrospun PVP-based scaffolds, and are generally attributed to a temporary metabolic recalibration associated with cell–material surface adaptation rather than cytotoxic insult. PVP is a well-characterized hydrophilic polymer widely used in biomedical applications owing to its low toxicity and favorable surface wettability; nevertheless, initial cell contact with its fibrous architecture has been associated with transient cytoskeletal reorganization that may transiently affect metabolic activity as measured by WST-1. Critically, the attenuation of this effect in the PBNF group compared with the PB group argues against a simple additive relationship between nanofiber and postbiotic components. Instead, it points toward a controlled-release mechanism wherein PVP nanofiber encapsulation modulates the kinetics of postbiotic exposure, thereby preventing the abrupt concentration surges that may underlie the more pronounced viability fluctuations observed in the PB group. This interpretation aligns with the broader literature on electrospun PVP-based delivery systems, which have consistently demonstrated the capacity to attenuate burst-release phenomena and stabilize bioactive molecule presentation at the cell–material interface.[26]

Importantly, the PNF group itself demonstrated a biologically non-negligible effect on cellular behavior. The concentration-dependent morphological compaction and mild viability fluctuations observed in PNF-treated cells suggest that the PVP scaffold, independent of its postbiotic cargo, is capable of eliciting a low-level cellular response. This finding has direct implications for the interpretation of PBNF data: the biological effects observed in the combination group cannot be attributed solely to the postbiotic fraction, but rather reflect a composite material–cell interaction in which scaffold architecture and bioactive loading act in concert. Similar scaffold-intrinsic bioactivity has been reported for other hydrophilic electrospun systems and is generally considered a functionally relevant rather than adverse property,

particularly in skin-targeted applications where cell–matrix crosstalk is mechanistically important.[27]

The morphological findings further corroborate this interpretation. The concentration-dependent compaction observed in PBNF-treated L929 fibroblasts should not be conflated with cytotoxicity; rather, it may reflect cytoskeletal reorganization associated with matrix-sensing behavior in response to a structured bioactive microenvironment. The preservation of characteristic spindle morphology across most tested concentrations, together with the absence of membrane disruption or detachment, substantiates the overall cytocompatibility of the system. The concordant findings in HaCaT keratinocytes further strengthen the translational relevance of these observations: as the primary cellular constituents of the epidermal barrier, keratinocytes represent a critical target population for any topically applied anti-aging formulation, and their tolerance of PBNF across the tested concentration range supports the suitability of this system for dermal application[28] (Figure 5-11).

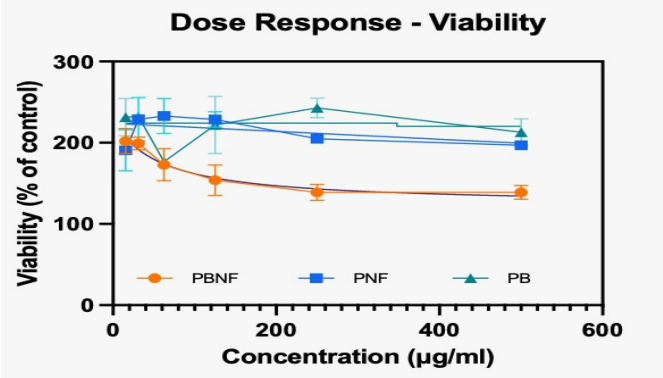

Figure 5. Dose response – Viability graph of PBNF, PNF, and PB-treated L929 cells after 24 hours of incubation
PBNF: Postbiotic-loaded nanofiber, PNF: Pure nanofiber, PB: Postbiotic

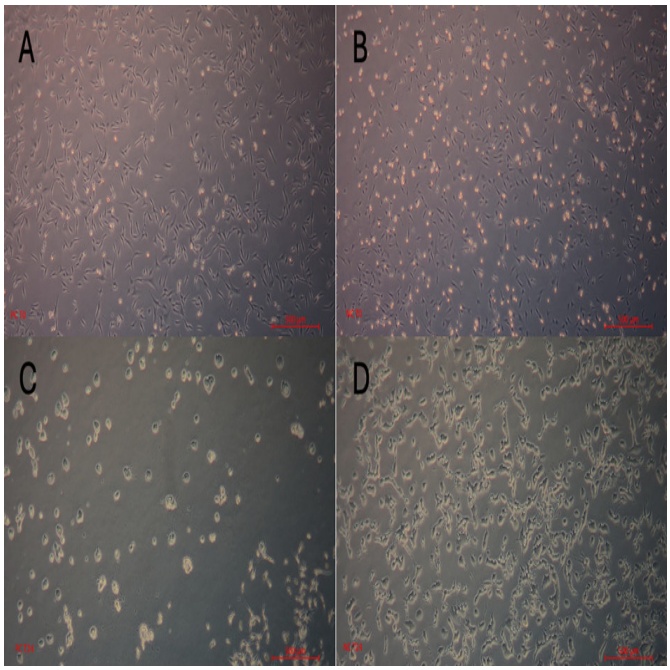

Figure 6. Control groups **(A, B, C, D).** Representative phase-contrast images of positive and negative control groups L929 fibroblasts at T0 and T24. (A: PC-T0, B: NC-T0, C: PC-T24, D: NC-T24)

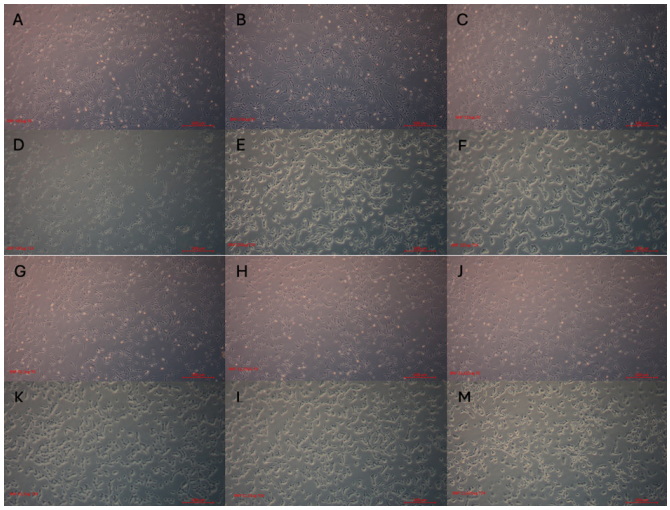

Figure 7. Pure nanofiber (PNF). Representative phase-contrast images of L929 fibroblasts cultured with empty nanofibers at concentrations ranging from 15.625 to 500 µg/ml at T0 and T24 (A:500 µg-T0, B: 250 µg-T0, C: 125 µg-T0, D: 500 µg-T24, E: 250 µg-T24, F: 125 µg-T24, G: 62,5 µg-T0, H: 31,25 µg-T0, J: 15,625 µg-T0, K: 62,5 µg-T24, L: 31,25 µg-T24, M: 15,625 µg-T24)

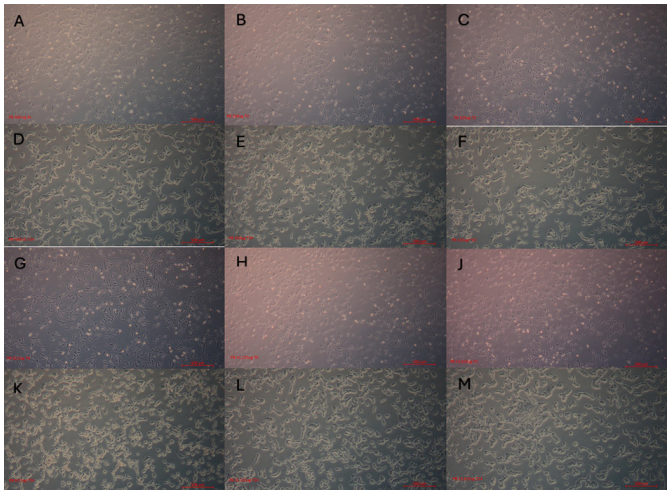

Figure 8. Postbiotic (PB). Representative phase-contrast images of L929 fibroblasts exposed to free postbiotic at concentrations of 15.625–500 µg/mL at T0 and T24. (A:500 µg-T0, B: 250 µg-T0, C: 125 µg-T0, D: 500 µg-T24, E: 250 µg-T24, F: 125 µg-T24, G: 62,5 µg-T0, H: 31,25 µg-T0, J: 15,625 µg-T0, K: 62,5 µg-T24, L: 31,25 µg-T24, M: 15,625 µg-T24).

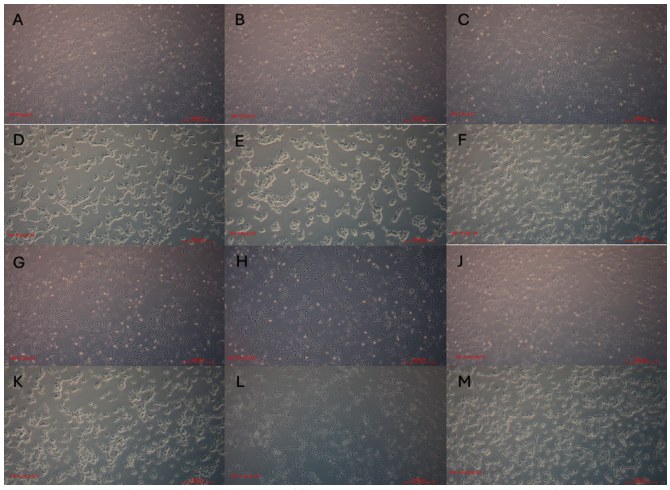

Figure 9. Postbiotic-loaded nanofiber (PBNF). Representative phase-contrast images of L929 fibroblasts treated with postbiotic-loaded nanofibers at concentrations ranging from 15.625 to 500 µg/mL at T0 and 24 hours (T24). (A:500 µg-T0, B: 250 µg-T0, C: 125 µg-T0, D: 500 µg-T24, E: 250 µg-T24, F: 125 µg-T24, G: 62,5 µg-T0, H: 31,25 µg-T0, J: 15,625 µg-T0, K: 62,5 µg-T24, L: 31,25 µg-T24, M: 15,625 µg-T24)

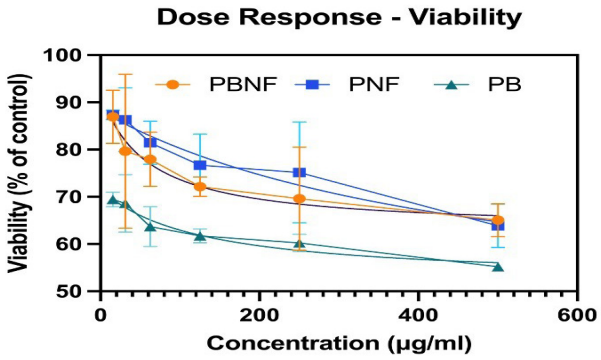

Figure 10. Dose response–viability graph of PBNF, PNF, and PB-treated HaCaT cells after 24 hours of incubation
PBNF: Postbiotic-loaded nanofiber, PNF: Pure nanofiber, PB: Postbiotic

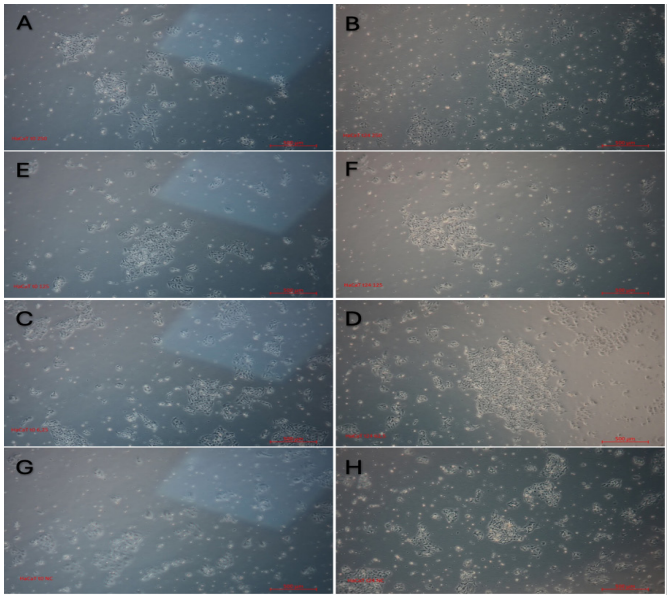

Figure 11. Postbiotic-loaded nanofiber (PBNF). Representative phase-contrast images of HaCaT keratinocytes treated with postbiotic-loaded nanofibers at concentrations ranging from 62.5 to 250 µg/ml at T0 and 24 hours (T24). (A:250 µg-T0, B: 250 µg-T24, C: 125 µg-T0, D: 125 µg-T24, E: 62.5 µg-T20, F: 62.5 µg-T24, G: NC-T0, H: NCT24

Gene Expression Analysis (qPCR)

The gene expression data provide a more mechanistically informative perspective on the biological activity of the tested formulations, and are particularly relevant given the anti-aging and skin rejuvenation context of the present study in Figure 12. The reciprocal transcriptional regulation of MMP1 and COL1A1, suppressed MMP1 expression concurrent with enhanced COL1A1 gene transcription, is directionally consistent with a pro-matrix, anti-degradative fibroblast phenotype, a profile of considerable interest in the context of dermal aging.

In aged or photoaged skin, the progressive decline in extracellular matrix integrity is mechanistically linked to the upregulation of MMP1, which mediates collagen fibril cleavage, alongside a concurrent reduction in COL1A1-driven collagen neosynthesis. The coordinated reversal of this pattern observed here, most prominently in postbiotic-containing groups and especially in PBNF, suggests that *Lactobacillus*-derived postbiotic constituents may engage transcriptional pathways governing matrix turnover in dermal fibroblasts.

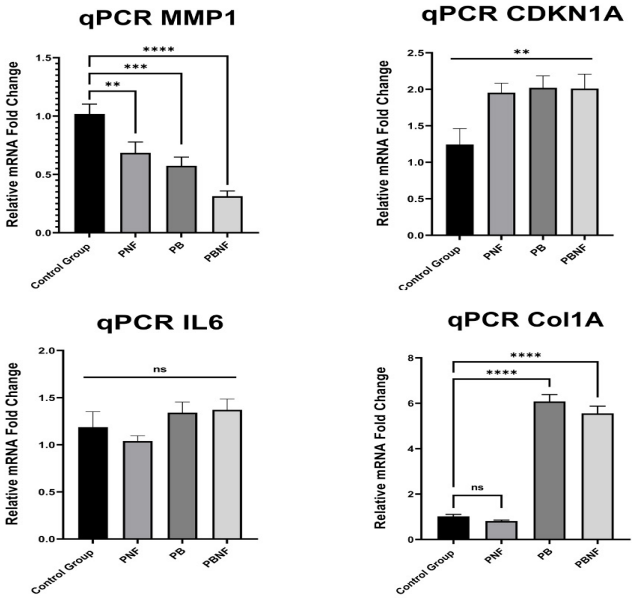

Figure 12. Relative mRNA expression levels of MMP1, COL1A1, CDKN1A, and IL6 determined by qPCR analysis in control, PNF, PB, and PBNF groups. Data are presented as mean±standard deviation (SD) from at least three independent experiments. Statistical significance was determined using appropriate statistical tests (*p<0.05, **p<0.01, ***p<0.001).
PBNF: Postbiotic-loaded nanofiber, PNF: Pure nanofiber, PB: Postbiotic

Lactobacillus-derived postbiotics, which encompass cell wall fragments, secreted peptides, exopolysaccharides, and short-chain metabolic byproducts, have been reported to modulate fibroblast behavior through Toll-like receptor 2 (TLR2)-mediated signaling and NF-κB pathway regulation, pathways known to influence both MMP and collagen gene expression. While the precise molecular intermediaries were not directly assessed in the present study, the transcriptional profile observed is mechanistically consistent with such receptor-mediated activity. Furthermore, the fact that the most pronounced MMP1 suppression was observed in the PBNF group, rather than in the postbiotic-only condition, suggests that nanofiber-mediated sustained delivery may optimize the temporal profile of postbiotic–receptor interactions, potentially by maintaining bioactive molecule concentrations within a functionally effective window over the exposure period.[29]

PNF group presented a distinct and noteworthy transcriptional signature. While COL1A1 expression in PNF-treated cells remained comparable to the control, CDKN1A was significantly elevated, mirroring the pattern observed in postbiotic-containing groups. This finding confirms that CDKN1A induction is not exclusively attributable to the postbiotic fraction and implicates the PVP scaffold itself as a stimulus capable of activating stress-responsive or cell cycle regulatory signaling. CDKN1A encodes p21^(Waf1/Cip1), a multifunctional cyclin-dependent kinase inhibitor whose expression is induced by a broad range of stimuli, including DNA damage, oxidative stress, and contact with foreign surfaces. Its induction in the context of nanofiber exposure, in the absence of morphological cytotoxicity, is most parsimoniously interpreted as a hormetic or adaptive stress response, a sub-lethal signaling event that activates protective cellular programs without compromising viability.

This interpretation is consistent with the growing literature on biomaterial-induced cellular adaptation, wherein transient p21 induction has been associated with subsequent proliferative recovery and enhanced matrix-synthetic activity rather than permanent growth arrest.[30]

The absence of significant IL-6 modulation across all experimental groups warrants careful consideration. IL-6 is a pleiotropic cytokine with context-dependent roles in both pro-inflammatory signaling and regenerative processes; its lack of differential expression in the present model indicates that the tested formulations did not activate classical inflammatory cascades under the studied in vitro conditions. From a safety perspective, this is an encouraging observation, as sustained IL-6 elevation in dermal fibroblasts has been associated with the senescence-associated secretory phenotype (SASP) and chronic low-grade skin inflammation.[14] However, the absence of IL-6 induction should not be interpreted as evidence of a broadly anti-inflammatory effect, as other relevant mediators, including IL-1β, TGF-β1, and TNF-α, were not assessed in the present study and may contribute to aspects of the biological response not captured by the current gene panel.[31]

Limitations

Taken together, the molecular data are most accurately interpreted as evidence of preliminary extracellular matrix-modulating activity in dermal fibroblasts, directionally consistent with an anti-aging transcriptional profile, rather than as definitive proof of regenerative or rejuvenating efficacy. The findings nonetheless establish a biologically plausible mechanistic basis for further investigation and justify progression toward more comprehensive functional assays, including collagen protein quantification by ELISA or Sircol assay, MMP activity measurement via zymography, SA-β-galactosidase-based senescence profiling, and reactive oxygen species quantification, to more rigorously define the cosmetic and regenerative potential of PBNF.

CONCLUSION

This work has shown that the PBNFs generated from PG are a promising carrier for use in the under-eye region. The nanofibers were of uniform morphology with rapid disintegration times and diffusion-controlled release mechanisms, which were beneficial for effective postbiotic delivery. The in vitro studies verified that the proposed system was biocompatible, supporting cell viability and proliferation better than postbiotics or PNF. The loading of postbiotics into the nanofibers resulted in a predictable biological effect, with no cytotoxic reactions observed. In view of these findings, PBNFs appear to offer a promising new strategy for skin care using nanotechnology to manage the early signs of aging in the periorbital region. Moreover, the molecular data suggest that the system may modulate key cellular pathways involved in extracellular matrix turnover and anti-aging processes, providing a foundation for further investigation into its regenerative potential. This study establishes a biologically plausible basis for the continued exploration of postbiotic-loaded nanofibers in cosmetic and regenerative applications.

ETHICAL DECLARATIONS

Ethics Committee Approval

Since this study involved the use of materials, approval from an ethics committee was not required.

Informed Consent

Since this was a material study, informed consent was not required.

Peer Review Process

This manuscript was subject to external peer review.

Conflict of Interest

The authors declare no conflicts of interest related to this study.

Financial Disclosure

The authors received no financial support for the conduct or publication of this research.

Author Contributions

Concept: MST, EG, HBY, GE, DB, AC, NCC, MEC; Design: MST, EG, HBY, GE, DB, AC, NCC, MEC; Control: MST, EG, HBY, GE, DB, AC, NCC, MEC; Resources: MST, EG, HBY, GE, DB, AC, NCC, MEC; Materials: MST, EG, HBY, GE, DB, AC, NCC, MEC; Data Collection and/or Processing: MST, EG, HBY, GE, DB, AC, NCC; Analysis and/or Interpretation: MST, EG, HBY, GE, DB, AC, NCC, MEC; Literature Review: MST, EG, HBY, GE, DB, AC, NCC; Writing the Article: MST, EG, HBY, GE, DB, AC, NCC, MEC; Critical Review: MST, EG, HBY, GE, DB, AC, NCC, MEC.

Acknowledgement

We would like to thank the owner of Shymeriae Biotechnology, Leyla Tarhan Celebi, for providing postbiotics to our study.

REFERENCES

1. Jeng L, Mirchandani A. Chapter 20-Skin health: what damages and ages skin? Evidence-based interventions to maintain healthy skin. In: Short E, ed. A Prescription for Healthy Living. Academic Press; 2021:225-233. doi:10.1016/B978-0-12-821573-9.00020-5
2. Park K. Role of micronutrients in skin health and function. *Biomol. Ther. (Seoul)*. 2015;23(3):207-217. doi:10.4062/biomolther.2015.003
3. Rostami F, Yekrang J, Gholamshahbazi N, Ramyar M, Dehghanniri P. Under-eye patch based on PVA-gelatin nanocomposite nanofiber as a potential skin care product for fast delivery of the coenzyme Q10 anti-aging agent: in vitro and in vivo studies. *Emerg. Mater.* 2023;6(6):1903-1921. doi:10.1007/s42247-023-00587-9
4. Bellu E, Garroni G, Cruciani S, et al. Smart nanofibers with natural extracts prevent senescence patterning in a dynamic cell culture model of human skin. *Cells*. 2020;9(12):2530. doi:10.3390/cells9122530
5. Yiğit İK, Türsen Ü, Türsen B, Solak B, Bakay ÖSK, Kroumpouzos G. Probiotics for skin aging and skin conditions in the elderly. *Clin. Dermatol.* 2026. doi:10.1016/j.clindermatol.2026.02.016
6. Cardoso AJR, Carvalho SG, Mantovanelli VR, et al. Postbiotics: modulation of the gut microbiota and potential for association with nanotechnology. *Probiotics Antimicrob Proteins*. 2025:1-19. doi:10.1007/s12602-025-10675-3
7. Liu H, Bai Y, Huang C, et al. Recent progress of electrospun herbal medicine nanofibers. *Biomol*. 2023;13(1):184. doi:10.3390/biom13010184

8. Kurakula M, Rao GK. Pharmaceutical assessment of polyvinylpyrrolidone (PVP): as excipient from conventional to controlled delivery systems with a spotlight on COVID-19 inhibition. *J Drug Deliv Sci Technol*. 2020;60: 102046. doi:10.1016/j.jddst.2020.102046
9. Doustdar F, Ghorbani M. ZIF-8 enriched electrospun ethyl cellulose/ polyvinylpyrrolidone scaffolds: the key role of polyvinylpyrrolidone molecular weight. *Carbohydr Polym*. 2022;291:119620. doi:10.1016/j.carbpol.2022.119620
10. Aguilar-Toalá J, Garcia-Varela R, Garcia H, et al. Postbiotics: an evolving term within the functional foods field. *Trends Food Sci Technol*. 2018;75: 105-114. doi:10.1016/j.tifs.2018.03.009
11. Zendeboodi F, Khorshidian N, Mortazavian AM, da Cruz AG. Probiotic: conceptualization from a new approach. *Curr Opin Food Sci*. 2020;32: 103-123. doi:10.1016/j.cofs.2020.03.009
12. Salminen S, Collado MC, Endo A, et al. The International Scientific Association of Probiotics and Prebiotics (ISAPP) consensus statement on the definition and scope of postbiotics. *Nat Rev Gastroenterol Hepatol*. 2021;18(9):649-667. doi:10.1038/s41575-021-00440-6
13. Nataraj BH, Ali SA, Behare PV, Yadav H. Postbiotics-parabiotics: the new horizons in microbial biotherapy and functional foods. *Microb Cell Fact*. 2020;19(1):168. doi:10.1186/s12934-020-01426-w
14. Cam ME, Ertas B, Alenezi H, et al. Accelerated diabetic wound healing by topical application of combination oral antidiabetic agents-loaded nanofibrous scaffolds: an in vitro and in vivo evaluation study. *Mater Sci Eng C*. 2021;119:111586. doi:10.1016/j.msec.2020.111586
15. Yekeler HB, Kabaoglu I, Guler E, et al. A comparison of electrospinning and pressurized gyration: production of empagliflozin-loaded polylactic acid/polycaprolactone fibrous patches. *J R Soc Interface*. 2025;22(224): 20240635. doi:10.1098/rsif.2024.0635
16. Ácsová A, Hojerová J, Martiniaková S. Efficacy of postbiotics against free radicals and UV radiation. *Chem Pap*. 2022;76(4):2357-2364. doi:10.1007/s11696-021-02018-7
17. Maleki M, Mehrabi M, Mehrabi M, Malvajerd SS. Comparative kinetic modeling and mathematical analysis of monoterpene release from nanocarrier systems. *AAPS PharmSciTech*. 2026;27(3):118. doi:10.1208/s12249-026-03332-7
18. Naig PJE, Kuo Z-Y, Wu Y-S, Hung K-Y. Electrospun carbon black-incorporated nanofibers for enhanced facial sebum adsorption. *IEEE*. 2025:104-108. doi:10.1109/NANOMED68094.2025.11431377
19. Guler E, Yekeler HB, Abobakr FKM, et al. In vitro and in vivo evaluation of rectal delivery of novel sulfasalazine-loaded hydrogels and nanofibers for enhanced ulcerative colitis therapy. *J Drug Deliv Sci Technol*. 2025: 107960. doi:10.1016/j.jddst.2025.107960
20. Guan H, Yang K. RNA isolation and real-time quantitative RT-PCR. *Methods Mol Biol*. 2008;456:259-270. doi:10.1007/978-1-59745-245-8_19
21. Guler E, Yekeler HB, Parviz G, et al. Vitamin B12-loaded chitosan-based nanoparticle-embedded polymeric nanofibers for sublingual and transdermal applications: two alternative application routes for vitamin B12. *Int J Biol Macromol*. 2024;258:128635. doi:10.1016/j.ijbiomac.2023.128635
22. Krithika R, Balasasirekha R. FTIR spectrum and XRD of postbiotics-exopolysaccharides zinc oxide nanoparticles. *J Adv Sci Res*. 2021;12(03 Suppl 2):292-300. doi:10.55218/JASR.s2202112334
23. Siepmann J, Peppas NA. Higuchi equation: derivation, applications, use and misuse. *Int J Pharm*. 2011;418(1):6-12. doi:10.1016/j.ijpharm.2011.03.051
24. Veysanoglu S, Ertas B, Guler E, et al. In vitro and in vivo evaluation of multi-target-directed Rivastigmine/Memantine/Gingko biloba-loaded nanofibers against Alzheimer's disease. *J Drug Deliv Sci Technol*. 2023; 86:104691. doi:10.1016/j.jddst.2023.104691
25. Kiňová Sepová H, Florová B, Bilková A, Drobná E, Březina V. Evaluation of adhesion properties of lactobacilli probiotic candidates. *Monatsh Chem*. 2018;149(5):893-899. doi:10.1007/s00706-017-2135-1
26. Cesur NP, Zad Ghaffari Vahdat K, Türkoğlu Laçin N. Fabrication of bacterial cellulose/PVP nanofiber composites by electrospinning. *Biopolymers*. 2024;115(5):e23606. doi:10.1002/bip.23606
27. Machado P, Ribeiro FN, Giublin FC, et al. Next-generation wound care: a scoping review on probiotic, prebiotic, synbiotic, and postbiotic cutaneous formulations. *Pharmaceuticals*. 2025;18(5):704. doi:10.3390/ph18050704
28. Lee JY, Park JY, Jeong Y, Kang CH. Anti-inflammatory response in TNFα/IFNγ-induced HaCaT keratinocytes and probiotic properties of *Lacticaseibacillus rhamnosus* MG4644, *Lacticaseibacillus paracasei* MG4693, and *Lactococcus lactis* MG5474. *J Microbiol Biotechnol*. 2023; 33(8):1039-1049. doi:10.4014/jmb.2301.01028
29. Park J-Y, Lee JY, Kim Y, Kang C-H. Lactic acid bacteria improve the photoprotective effect via MAPK/AP-1/MMP signaling pathway on skin fibroblasts. *Microorganisms*. 2022;10(12):2481. doi:10.3390/microorganisms10122481
30. Ul Hassan MH, Shahbaz M, Imran M, et al. Isoflavones: promising natural agent for cancer prevention and treatment. *Food Sci Nutr Mar*. 2025;13(3):e70091. doi:10.1002/fsn3.70091
31. Kishimoto M, Nomoto R, Mizuno M, Osawa R. An in vitro investigation of immunomodulatory properties of *Lactobacillus plantarum* and *L. delbrueckii* cells and their extracellular polysaccharides. *Biosci Microbiota Food Health*. 2017;36(3):101-110. doi:10.12938/bmfh.17-001